

Methyl(hydrido)platinum(IV) Complexes: X-ray Structure of the First (μ -Hydrido)diplatinum(IV) Complex

Geoffrey S. Hill, Jagadese J. Vittal, and Richard J. Puddephatt*

Department of Chemistry, The University of Western Ontario,
London, Ontario, Canada N6A 5B7

Received November 18, 1996[®]

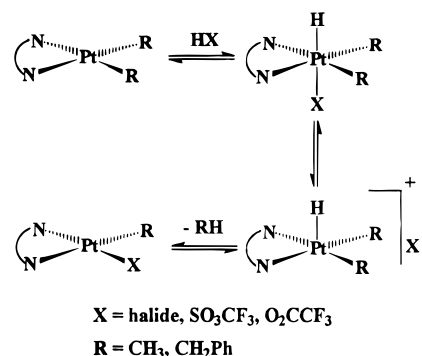
The complex *fac*-[PtMe₃(SO₃CF₃)(bu₂bpy)] (**1**) (bu₂bpy = 4,4'-di-*tert*-butyl-2,2'-bipyridine) reacts with NaBH₄ to give [Pt₂(μ -H)Me₆(bu₂bpy)₂](SO₃CF₃) (**2**), which is the first example of a (μ -hydrido)diplatinum(IV) complex. Complex **2** was fully characterized on the basis of microanalytical, ¹H and ¹⁹⁵Pt NMR spectroscopic, and X-ray crystallographic data. The reaction of **1** with a large excess of NaBH₄ results in the formation of an equilibrium mixture of **2** and *fac*-[PtHMe₃(bu₂bpy)] (**3**). Complex **3** was characterized by ¹H NMR spectroscopy in solution but could not be isolated in pure form due to the ease of reversion to **2**. Both complexes **2** and **3**, which have no ligand that can easily dissociate, are thermally stable to reductive elimination of methane (both in solution and, in the case of complex **2**, in the solid state) and to isotopic exchange within Pt(D)CH₃ groups, thus giving strong support to the theory that both reactions must occur from within a five-coordinate intermediate. Complex **2** reacts slowly with HX (HX = HCl, HO₂CCF₃, HSC₆H₅, NH₄⁺) to give either 2 equiv of *fac*-[PtClMe₃(bu₂bpy)] (**4**), *fac*-[PtMe₃(O₂CCF₃)(bu₂bpy)] (**5**), and *fac*-[PtMe₃(NH₃)(bu₂bpy)](SO₃CF₃) (**6**) or 1 equiv of [Pt₂(μ -SC₆H₅)Me₆(bu₂bpy)₂](SO₃CF₃) (**7**), respectively. Qualitatively, the relative rates of these reactions follow the order of acid strength, i.e. HCl \approx HO₂CCF₃ \gg HSC₆H₅, indicating that the rate-determining step involves electrophilic attack of H⁺ on **2**. Complex **2** reacts very slowly with nucleophiles such as PPh₃ to give 1 equiv of *fac*-[PtMe₃(PPh₃)(bu₂bpy)](SO₃CF₃) (**8**) and 1 equiv of **3**. The reaction of CCl₄ with **2** gives *fac*-[PtClMe₃(bu₂bpy)] (**4**), [PtCl₂Me₂(bu₂bpy)] (**11**), and *mer*-[PtCl₃Me(bu₂bpy)] (**12**) in a 1.0:0.8:0.2 product ratio but without formation of chloroform.

Introduction

Several research groups have recently reported the first examples of a fundamentally important class of organometallic compounds, alkyl(hydrido)platinum(IV) complexes.¹ These complexes are proposed intermediates in the protonolysis of the Pt–C bond and in alkane activation by Pt(II). In most of these reports, complexes of formula [PtH(X)R₂(NN)] (X = halide, O₂CCF₃, SO₃CF₃; R = CH₃, CH₂Ph; NN = a bidentate nitrogen-donor ligand) are formed by the *trans* oxidative addition of HX to the corresponding dialkylplatinum(II) complex, [PtR₂(NN)],¹ and are usually characterized only *in situ* by low-temperature ¹H NMR spectroscopy because, at room temperature, they rapidly decompose.^{1a,d–e} The proposed mechanism of this decomposition involves initial dissociation of the ligand *trans* to the hydride (X[–]), to give the five-coordinate intermediate [PtHR₂(NN)]⁺ which then easily reductively eliminates alkane (Scheme 1).

This suggests that a complex where all ligands are strongly bound, such as [PtH(X)Me₂(NN)], where X cannot easily dissociate from platinum, would be stable to the reductive elimination of CH₄. This principle was recognized recently by two research groups who re-

Scheme 1



ported examples of methyl(hydrido)platinum(IV) complexes that are truly stable to the reductive elimination of CH₄ of the type [PtHMe₂(NN'N'')] {NN'N'' = a tris-(pyrazolyl)borate ligand}.^{1b,c} In these complexes, the ligand *trans* to hydride is a strongly coordinating pyrazolyl group of the NN'N'' ligand. In this work, the aim of isolating a stable methyl(hydrido)platinum(IV) complex is the same, but the approach was different. The objective was to synthesize the complex *fac*-[PtHMe₃(bu₂bpy)] (bu₂bpy = 4,4'-di-*tert*-butyl-2,2'-bipyridine). This complex should have no easily dissociated group and so should be stable to reductive elimination, but it should possess interesting reaction chemistry since it contains mutually *trans* methyl and hydrido ligands (both with large *trans* effects) leading to stronger hydridic character than in the pyrazolylborate complexes discussed above. By analogy, the mutually *trans*

[®] Abstract published in *Advance ACS Abstracts*, February 15, 1997.

(1) (a) Stahl, S. S.; Labinger, J. A.; Bercaw, J. E. *J. Am. Chem. Soc.* **1996**, *118*, 5961. (b) O'Reilly, S. A.; White, P. S.; Templeton, J. L. *J. Am. Chem. Soc.* **1996**, *118*, 5684. (c) Canty, A. J.; Dedieu, A.; Jin, H.; Milet, A.; Richmond, M. K. *Organometallics* **1996**, *15*, 2845. (d) Hill, G. S.; Rendina, L. M.; Puddephatt, R. J. *Organometallics* **1995**, *14*, 4966. (e) De Felice, V.; De Renzi, A.; Panunzi, A.; Tesaro, D. *J. Organomet. Chem.* **1995**, *488*, C13.

Table 1. Selected ^1H NMR Spectroscopic Data for Complexes 1–12^e

complex	$\delta(^1\text{H})$			
	Pt–Me ^a	Pt–Me ^b	^t Bu	other
1 ^c	0.64 [s, 3H, $^2J(\text{PtH}) = 87.0$ Hz]	1.21 [s, 6H, $^2J(\text{PtH}) = 66.5$ Hz]	1.49 (s, 18H)	
2 ^d	0.13 [s, 6H, $^2J(\text{PtH}) = 65.9$ Hz]	0.47 [s, 12H, $^2J(\text{PtH}) = 69.6$ Hz]	1.49 (s, 36H)	–11.7 [s, 1H, $^1J(\text{PtH}) = 442$ Hz, Pt–H]
3 ^c	–0.79 [s, 3H, $^2J(\text{PtH}) = 43.0$ Hz]	0.75 [s, 6H, $^2J(\text{PtH}) = 66.0$ Hz]	1.48 (s, 18H)	–7.0 [s, 1H, $^1J(\text{PtH}) = 8.5$ Hz, Pt–H]
4 ^c	0.36 [s, 3H, $^2J(\text{PtH}) = 74.5$ Hz]	1.99 [s, 6H, $^2J(\text{PtH}) = 69.7$ Hz]	1.46 (s, 18H)	
5 ^c	0.34 [s, 3H, $^2J(\text{PtH}) = 76.4$ Hz]	1.98 [s, 6H, $^2J(\text{PtH}) = 67.4$ Hz]	1.46 (s, 18H)	
6 ^d	0.31 [s, 3H, $^2J(\text{PtH}) = 71.5$ Hz]	1.04 [s, 6H, $^2J(\text{PtH}) = 67.8$ Hz]	1.47 (s, 18H)	2.30 [br s, 3H, $^2J(\text{PtH}) = \text{ca. } 17.5$ Hz, Pt–NH ₃]
7 ^c	0.36 [s, 6H, $^2J(\text{PtH}) = 69.8$ Hz]	1.15 [s, 12H, $^2J(\text{PtH}) = 69.3$ Hz]	1.37 (s, 36H)	6.55 [t, 1H, <i>p</i> -SC ₆ H ₅], 6.11 [dd, 2H, <i>m</i> -SC ₆ H ₅], 5.43 [d, 2H, <i>o</i> -SC ₆ H ₅]
8 ^c	0.65 [s, 6H, $^2J(\text{PtH}) = 44.0$ Hz]	0.84 [s, 6H, $^2J(\text{PtH}) = 72.0$ Hz]	1.49 (s, 18H)	
9 ^c	0.15 [s, 3H, $^2J(\text{PtH}) = 63.4$ Hz]	1.09 [s, 6H, $^2J(\text{PtH}) = 70.6$ Hz]	1.43 (s, 18H)	6.56 [m, 1H, <i>p</i> -SC ₆ H ₅], 6.35 [m, 2H, <i>m</i> -SC ₆ H ₅], 6.32 [m, 2H, <i>o</i> -SC ₆ H ₅]
10 ^c	0.52 [s, 3H, $^2J(\text{PtH}) = 59.8$ Hz]	1.33 [s, 6H, $^2J(\text{PtH}) = 67.5$ Hz]	1.44 (s, 18H)	
11 ^c		1.85 [s, 6H, $^2J(\text{PtH}) = 69.5$ Hz]	1.46 (s, 18H)	
12 ^c		2.69 [s, 3H, $^2J(\text{PtH}) = 68.0$ Hz]	1.50 (s, 9H)	
			1.49 [s, 9H]	

^a Pt–Me *cis* to bu₂bpy. ^b Pt–Me *trans* to bu₂bpy. ^c In acetone-*d*₆. ^d In CD₂Cl₂. ^e Quoted multiplicities do not include ¹⁹⁵Pt satellite signals.

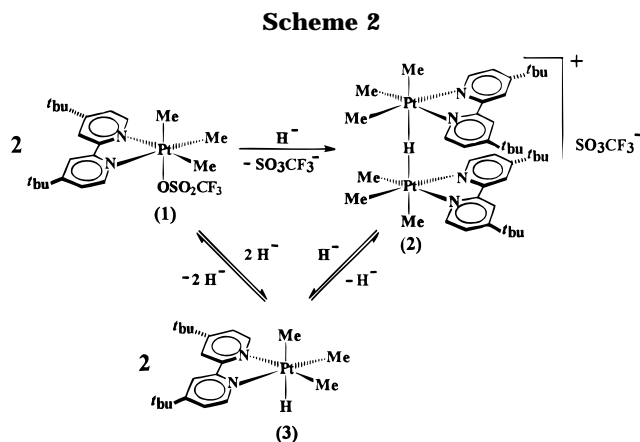
methyl ligands in the tetramethylplatinum(IV) complex [PtMe₄(bpy)] (bpy = 2,2'-bipyridine) have been shown to readily react with a variety of electrophilic and unsaturated reagents.² It will be seen that the desired complex *fac*-[PtHMe₃(bu₂bpy)] could be generated in solution by reaction of *fac*-[PtMe₃(SO₃CF₃)(bu₂bpy)] (1) with NaBH₄, but the major product proved to be the binuclear cationic complex, [Pt₂(μ-H)Me₆(bu₂bpy)₂]⁺SO₃CF₃[–] (2), which is the first example of a (μ-hydrido)-diplatinum(IV) complex and which is shown to have interesting properties. A portion of this work has been reported in an earlier communication.³

Results and Discussion

Synthesis and Characterization of [Pt₂(μ-H)Me₆(bu₂bpy)₂]⁺SO₃CF₃[–] (2). The reaction of [PtMe₂(bu₂bpy)] with MeOSO₂CF₃ in diethyl ether solution quantitatively affords *fac*-[PtMe₃(SO₃CF₃)(bu₂bpy)] (1) as an off-white solid. The ^1H NMR spectrum (acetone-*d*₆) of 1 shows the expected three sets of aromatic resonances and one *tert*-butyl resonance of the two equivalent pyridyl constituents of the bu₂bpy ligand. The two methylplatinum resonances appear in a 2:1 intensity ratio at $\delta = 1.21$ [$^2J(\text{PtH}) = 66.5$ Hz] and $\delta = 0.64$ [$^2J(\text{PtH}) = 87.0$ Hz], respectively (Table 1). These magnitudes of $^2J(\text{PtH})$ are typical for methylplatinum(IV) ligands *trans* to bu₂bpy and *trans* to SO₃CF₃ respectively.^{1d,4}

Treatment of *fac*-[PtMe₃(SO₃CF₃)(bu₂bpy)] (1) with NaBH₄ in THF solution affords the first binuclear platinum(IV) hydride complex [Pt₂(μ-H)Me₆(bu₂bpy)₂]⁺SO₃CF₃[–] (2), which was isolated as a yellow powder in 83% yield (Scheme 2).

The ^1H NMR spectrum (CD₂Cl₂) of complex 2 shows three aromatic resonances and one *tert*-butyl resonance due to the two equivalent pyridyl groups of the bu₂bpy ligand. These data rule out the alternative isomer with μ-H *trans* to nitrogen, which would have nonequivalent pyridyl groups. There are two methylplatinum reso-



nances in a 2:1 intensity ratio due to the methylplatinum groups *trans* to bu₂bpy [$\delta = 0.47$, $^2J(\text{PtH}) = 69.6$ Hz] and *trans* to hydride [$\delta = 0.13$, $^2J(\text{PtH}) = 65.9$ Hz], respectively (Table 1). Both peaks showed a small coupling with the hydrido ligand [$^3J(\text{HH}) = 1.0$ Hz in each case]. The most convincing ^1H NMR evidence for a bridging hydrido ligand comes from the low-frequency Pt–H resonance at $\delta = -11.7$ with $^1J(\text{PtH}) = 442$ Hz. The resonance appears as a 1:8:18:8:1 multiplet due to coupling to ¹⁹⁵Pt, thus proving the presence of a Pt₂(μ-H) group.⁵ This Pt–H resonance is absent in the ^1H NMR spectrum of [Pt₂(μ-D)Me₆(bu₂bpy)₂]⁺SO₃CF₃[–] (2*), prepared using NaBD₄. The $^2\text{H}\{^1\text{H}\}$ NMR spectrum (CH₂Cl₂) of complex 2* shows only the expected singlet at $\delta = -11.7$ with $^1J(\text{PtD}) = 68.4$ Hz.⁶ The ^1H -coupled ¹⁹⁵Pt NMR spectrum (THF-*d*₈) of 2 contains a doublet at $\delta = -1238$ due to coupling with the bridging hydrido ligand [$^1J(\text{PtH}) = 440$ Hz], thus proving the presence of only a single μ-H ligand. The ¹⁹⁵Pt NMR spectrum (CD₂Cl₂) of [Pt₂(μ-D)Me₆(bu₂bpy)₂]⁺SO₃CF₃[–] (2*) shows only a broad singlet at $\delta = -1240$, since the line width ($\Delta\nu^{1/2} = \text{ca. } 160$ Hz) is greater than the coupling $^1J(\text{PtD})$. The ^1H NMR spectrum of 2 is essentially unchanged from room temperature to –90 °C.

The proposed structure of [Pt₂(μ-H)Me₆(bu₂bpy)₂]⁺SO₃CF₃[–] (2) was confirmed by X-ray crystallography. An ORTEP diagram of 2 is shown in Figure 1, while Table 2 contains selected bond distances and angles. The X-ray molecular structure of 2·THF contains two very

(2) (a) Hux, J. E.; Puddephatt, R. J. *Inorg. Chim. Acta* **1985**, 100, 1. (b) Hux, J. E.; Puddephatt, R. J. *J. Organomet. Chem.* **1988**, 346, C31.

(3) Hill, G. S.; Puddephatt, R. J. *J. Am. Chem. Soc.* **1996**, 118, 8745.

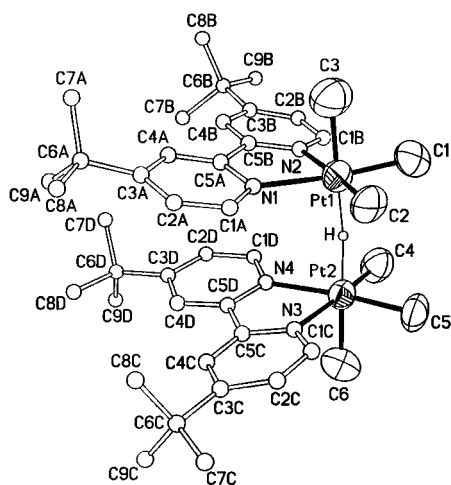
(4) For example, see: (a) Rendina, L. M.; Vittal, J. J.; Puddephatt, R. J. *Organometallics* **1995**, 14, 1030. (b) Anderson, C. M.; Crespo, M.; Jennings, M. C.; Lough, A. J.; Ferguson, G.; Puddephatt, R. J. *Organometallics* **1991**, 10, 2672. (c) Monaghan, P. K.; Puddephatt, R. J. *J. Chem. Soc., Dalton Trans.* **1988**, 595. (d) Crespo, M.; Puddephatt, R. J. *Organometallics* **1987**, 6, 2548. (e) Jawad, J.; Puddephatt, R. J. *J. Chem. Soc., Dalton Trans.* **1977**, 1466. (f) Kuypers, J. *Inorg. Chem.* **1977**, 16, 2171. (g) Jawad, J.; Puddephatt, R. J. *J. Organomet. Chem.* **1976**, 117, 297. (h) Appleton, T. G.; Clark, H. C.; Manzer, L. E. *Coord. Chem. Rev.* **1973**, 10, 335.

(5) (a) Brown, M. P.; Cooper, S. J.; Frew, A. A.; Manojlovic-Muir, L.; Muir, K. W.; Puddephatt, R. J.; Thompson, M. A. *J. Chem. Soc., Dalton Trans.* **1982**, 299. (b) Brown, M. P.; Puddephatt, R. J.; Rashidi, M.; Seddon, K. R. *J. Chem. Soc., Dalton Trans.* **1978**, 516.

(6) $\gamma_{\text{H}}/\gamma_{\text{D}} = 6.51 \approx ^1J(\text{PtH})/^1J(\text{PtD}) = 6.47$.

Table 2. Selected Bond Distances (Å) and Angles (deg) in $[\text{Pt}_2(\mu\text{-H})\text{Me}_6(\text{bu}_2\text{bpy})_2]\text{SO}_3\text{CF}_3\cdot\text{THF}$

(A) Bond Distances			
Pt(1)–H	1.69(2)	Pt(2)–H	1.70(2)
Pt(1)–Pt(2)	3.388(1)	Pt(2)–C(4)	2.02(2)
Pt(1)–C(1)	2.01(2)	Pt(2)–C(5)	2.05(1)
Pt(1)–C(2)	2.04(2)	Pt(2)–C(6)	2.11(2)
Pt(1)–C(3)	2.09(2)	Pt(2)–N(3)	2.15(1)
Pt(1)–N(1)	2.15(1)	Pt(2)–N(4)	2.15(1)
Pt(1)–N(2)	2.12(1)		
(b) Bond Angles			
Pt(1)–H–Pt(2)	173.5(71)	C(4)–Pt(2)–C(5)	87.5(7)
C(1)–Pt(1)–C(2)	87.0(7)	C(4)–Pt(2)–C(6)	88.6(8)
C(1)–Pt(1)–C(3)	88.9(7)	C(4)–Pt(2)–N(3)	173.8(6)
C(1)–Pt(1)–N(1)	173.2(6)	C(4)–Pt(2)–N(4)	97.7(6)
C(1)–Pt(1)–N(2)	98.9(5)	C(5)–Pt(2)–C(6)	89.6(8)
C(2)–Pt(1)–C(3)	89.1(7)	C(5)–Pt(2)–N(3)	98.1(6)
C(2)–Pt(1)–N(1)	98.4(6)	C(5)–Pt(2)–N(4)	174.2(6)
C(2)–Pt(1)–N(2)	174.0(6)	C(6)–Pt(2)–N(3)	89.0(6)
C(3)–Pt(1)–N(1)	87.1(7)	C(6)–Pt(2)–N(4)	88.1(6)
C(3)–Pt(1)–N(2)	89.6(6)	C(6)–Pt(2)–Pt(1)	176.8(6)
C(3)–Pt(1)–Pt(2)	177.8(6)	N(3)–Pt(2)–N(4)	76.6(4)
N(2)–Pt(1)–N(1)	75.7(4)		
(c) Torsion Angles			
C(1)–Pt(1)–Pt(2)–C(4)	–43.14(0.70)	N(1)–Pt(1)–Pt(2)–N(4)	33.80(0.45)
C(1)–Pt(1)–Pt(2)–C(5)	44.50(0.68)	N(2)–Pt(1)–Pt(2)–N(4)	–41.86(0.46)
C(2)–Pt(1)–Pt(2)–N(3)	55.65(0.62)	N(1)–C(5A)–C(5B)–N(2)	–2.94(1.82)
C(2)–Pt(1)–Pt(2)–C(5)	–42.52(0.76)	N(3)–C(5C)–C(5D)–N(4)	3.87(1.83)
N(2)–Pt(1)–Pt(2)–C(4)	55.77(0.61)	C(4A)–C(5A)–C(5B)–C(4B)	–6.84(2.26)
N(1)–Pt(1)–Pt(2)–N(3)	–42.75(0.43)	C(4C)–C(5C)–C(5D)–C(4D)	3.21(2.22)

**Figure 1.** ORTEP diagram of $[\text{Pt}_2(\mu\text{-H})\text{Me}_6(\text{bu}_2\text{bpy})_2]^+$ (**2**). Thermal ellipsoids show the 50% probability level. The hydrogen atoms of the methylplatinum and bu_2bpy ligands have been omitted for clarity. The disorder of the methyl groups at C(6c) is not shown.

similar *fac*- $[\text{PtMe}_3]$ units bridged by H. The lengths of the Pt(1)–C(1), Pt(1)–C(2), Pt(2)–C(4), and Pt(2)–C(5) bonds do not differ significantly [ranging from 2.01(2) to 2.047(2) Å] and are of typical magnitude for a methylplatinum(IV) ligand *trans* to bu_2bpy .⁷ The Pt–C bond lengths of the two methylplatinum ligands *trans* to hydride are very similar [Pt(1)–C(2) = 2.09(2) Å, Pt(2)–C(6) = 2.11(2) Å] and are longer than the methylplatinum ligands *trans* to bu_2bpy . Therefore, the μ -hydrido ligand has a larger *trans* influence than bu_2bpy . This agrees with the data obtained from the ^1H NMR spectrum of **2** in which the magnitude of $^2J(\text{PtH})$ for the Pt–Me ligands *trans* to bu_2bpy is slightly larger than for the Pt–Me ligands *trans* to hydride (Table 1).

The geometries at the platinum centers are close to octahedral. The only notable exceptions are the N(1)–

Pt(1)–N(2) and N(3)–Pt(2)–N(4) bond angles of 75.7(4) and 76.6(4)°, respectively, which depart significantly from the ideal 90° octahedral angle, due to the restricted bite of the bu_2bpy ligand.⁷

The sets of atoms Pt(1), C(1), C(2), N(1), N(2) and Pt(2), C(4), C(5), N(3), N(4) form well-defined planes (rms Δ = 0.030 and 0.012, respectively) that are nearly parallel to each other [angle between planes = 3.6(5)°]. The bonds in these two planes adopt a staggered conformation about the Pt(1)–Pt(2) vector such that the C(1)–Pt(1)–Pt(2)–C(5) torsion angle is 44.5(0.7)°. Furthermore, the two bu_2bpy ligands adopt a *syn* arrangement such that the centroid of the N(1)C(1A)C(2A)C(3A)–C(4A)C(5A) ring lies above the midpoint of the C(5C)–C(5D) bond. This arrangement minimizes the repulsions between the *tert*-butyl groups of adjacent bu_2bpy ligands while still maintaining a significant degree of π -stacking between the pyridyl groups. The bu_2bpy ligands show no exceptional features, and each consists of two planar rings (rms Δ < 0.018 Å for all four rings) that are twisted about the C–C single bonds such that the torsion angles for C(4B)–C(5B)–C(5A)–C(4A) and C(4C)–C(5C)–C(5D)–C(4D) are –6.84(2.26) and 3.21–(2.22)°, respectively. The two bu_2bpy ligands are significantly tilted from the corresponding PtMe_2N_2 planes and from one another (Figure 1). For example, the N(1)C(1A)C(2A)C(3A)C(4A)C(5A) and N(2)C(1B)C(2B)–C(3B)C(4B)C(5B) planes are tilted from the Pt(1)C(1)–C(2)N(1)N(2) plane by 16.5(8) and 13.2(8)°, respectively, and the N(3)C(1C)C(2C)C(3C)C(4C)C(5C) and N(4)–C(1D)C(2D)C(3D)C(4D)C(5D) planes are tilted from the Pt(2)C(4)C(5)N(3)N(4) plane by 12.2(8) and 8.7(6)°, respectively. This is most certainly a result of interligand repulsion of the *tert*-butyl groups of the bu_2bpy ligands. However, the observation of only single resonances for the *tert*-butyl protons and the MePt protons *trans* to nitrogen in **2** at –90 °C indicates that there is only a small barrier to rotation about the PtHPt axis.

The μ -hydrido ligand in **2** was successfully, though not accurately, located. Typically, M(μ -H)M bonds are

(7) For example, see: (a) Levy, C. J.; Vittal, J. J.; Puddephatt, R. J. *Organometallics* **1996**, *15*, 2108. (b) Rendina, L. M.; Vittal, J. J.; Puddephatt, R. J. *Organometallics* **1996**, *15*, 2108.

bent and are best represented as 3c–2e[−] bonds with a significant degree of concurrent M–M and M–H bonding.⁸ The observation of near linearity of the Pt(1)–H–Pt(2) angle [173(7)°] and of a large Pt(1)⋯Pt(2) separation [3.388(1) Å] indicates that there is very little, if any, Pt–Pt bonding in **2**.^{5a,9} The near linearity of the Pt–H–Pt group is probably a direct result of steric constraints due to the presence of the octahedral platinum centers.

Formation and Characterization of *fac*-[PtHMe₃(bu₂bpy)] (3**).** Reaction of complex **2** with a large excess of NaBH₄ results in the formation of an equilibrium mixture of **2** and 2 equiv of *fac*-[PtHMe₃(bu₂bpy)] (**3**) (Scheme 2). Attempts to isolate **3** were unsuccessful, since workup of the reaction mixtures leads to reversion to **2** as the excess borohydride is removed. Under the strongly basic conditions of its formation, the complex **3** decomposes slowly with precipitation of metallic platinum, but **3** survives for about a 1 at room temperature and was readily characterized by ¹H NMR spectroscopy (acetone-*d*₆). Again, the two equivalent bipyridine moieties of the bu₂bpy give rise to three aromatic and one *tert*-butyl resonance. The methylplatinum resonances appear in a 2:1 intensity ratio at δ = 0.75 (*trans* to bu₂bpy) and −0.79 (*trans* to H) with ²*J*(PtH) = 66.0 and 43.0 Hz, respectively (Table 1). Note that the methyl group *trans* to the hydrido ligand has a very low coupling constant to ¹⁹⁵Pt (43.0 Hz), which is significantly smaller than that of the methylplatinum ligand *trans* to the bridging hydride in complex **2** [²*J*(PtH) = 65.9 Hz] but is similar to that of the mutually *trans* methylplatinum ligands in [PtMe₄(NN)] [²*J*(PtH) = 44 Hz; NN = bpy, bu₂bpy]. Thus the terminal hydrido ligand in complex **3** has a stronger *trans* influence than the bridging hydride in **2**. The Pt–H ligand resonates at δ = −7.0 with ¹*J*(PtH) = 805 Hz. This resonance appears as a 1:4:1 multiplet due to coupling to ¹⁹⁵Pt, thus proving the presence of a terminal Pt–H group. This coupling constant is approximately twice the magnitude of that found in **2**, which is reasonable since the s-electron density of the hydride is shared between two platinum centers in **2**. Nevertheless, the value of ¹*J*(PtH) for complex **3** is still significantly smaller than that of [PtH(X)Me₂(bu₂bpy)] (X = Cl, Br, I; ¹*J*(PtH) = 1589.7, 1630.5, 1655.5 Hz, respectively) again illustrating the *trans*-effect of the *trans* methyl ligand.^{1d} It is the strong σ -donor effect of the *trans*-methyl group in **3** which is expected to lead to hydridic character of the Pt–H group in **3** compared to the complexes such as [PtHClMe₂(bu₂bpy)]. It is presumably this hydridic character of the Pt–H bond that leads to the reaction of **3** with **1** with displacement of SO₃CF₃ to give the stable complex **2**. This methodology, where a hydridic M–H group ligates to a second metal, M', to give a M–H–M' system, has been exploited before.¹⁰

Thermal Decomposition Studies of Complexes **2 and **3**.** The complex *fac*-[PtHMe₃(bu₂bpy)] (**3**) was not isolable so a detailed investigation of its thermal stability was not possible. Nevertheless, **3** appears to be

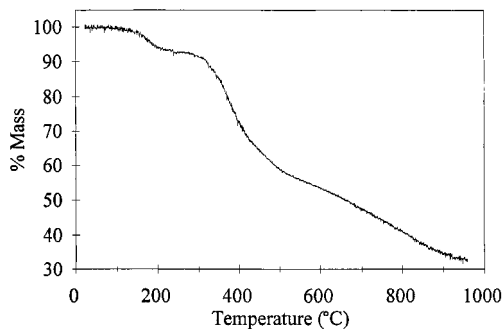


Figure 2. Thermogravimetric analysis (TGA) curve showing the thermal decomposition of [Pt₂(μ-H)Me₆(bu₂bpy)₂]·SO₃CF₃ (**2**).

stable to reductive elimination of methane since at no time during the synthesis of **3** is [PtMe₂(bu₂bpy)] (the reductive elimination product) produced.¹¹ [PtMe₂(bu₂bpy)] is stable to NaBH₄, so its absence in the reaction mixture confirms the stability of **3** to reductive elimination of CH₄. Complex **2** is stable in chlorinated solvents for several days at room temperature after which it slowly decomposes to *fac*-[PtClMe₃(bu₂bpy)] (**4**) (see later). Room-temperature solutions of complex **2** in nonchlorinated solvents are indefinitely stable and only start to decompose (precipitating metallic platinum) at temperatures in excess of 90 °C (toluene solution). The solid-state decomposition of complex **2** was studied by thermogravimetric analysis (TGA). A typical TGA plot is shown in Figure 2 and confirms that **2** is very resistant to reductive elimination. Complex **2** is stable to ca. 175 °C after which it undergoes a clean 8% mass loss. This mass loss corresponds approximately to elimination of all methyl and hydride ligands. The gaseous products of this elimination were analyzed by GC-MS and were found to be composed of mainly CH₄ and traces of C₂H₆. Complex **2** undergoes a further decomposition between ca. 325 °C and ca. 950 °C to ultimately leave metallic platinum (33% mass residue).

The only other TGA analysis of an alkyl(hydrido)platinum(IV) complex was of [PtHMe₂(Tp')] [Tp' = hydridotris(3,5-dimethylpyrazolyl)borate].^{1b} It was found that this complex decomposes at 190 °C, to give unidentified products. Recently it was shown that a similar complex, [PtHMe₂{(pz)₃BH}] [(pz)₃BH = tris(pyrazol-1-yl)borate] decomposes at 140 °C in toluene solution to form metallic platinum and CH₄.^{1c} No solid-state decomposition studies of this complex have been reported.

In all of the above examples of methyl(hydrido)platinum(IV) complexes that are resistant to reductive elimination of CH₄ [i.e. [PtHMe₂(NN'N'')] (NN'N'' = Tp', (pz)₃BH), [Pt₂(μ-H)Me₆(bu₂bpy)₂]SO₃CF₃ (**2**), *fac*-[PtHMe₃(bu₂bpy)] (**3**)] the ligand *trans* to hydride cannot easily dissociate. Presumably, it is the absence of ligands that can easily dissociate that explains the extraordinary thermal stability of these complexes. These results give further support for the proposed decomposition pathway of alkyl(hydrido)platinum(IV) complexes in Scheme 1.

Isotopic Exchange within Pt(D)CH₃ Groups. Very recently, it was shown that the protonolysis of the Pt–C bond by DCl in [PtMe₂(tmeda)] (tmeda = *N,N,N,N*-tetramethylethylenediamine) proceeds through

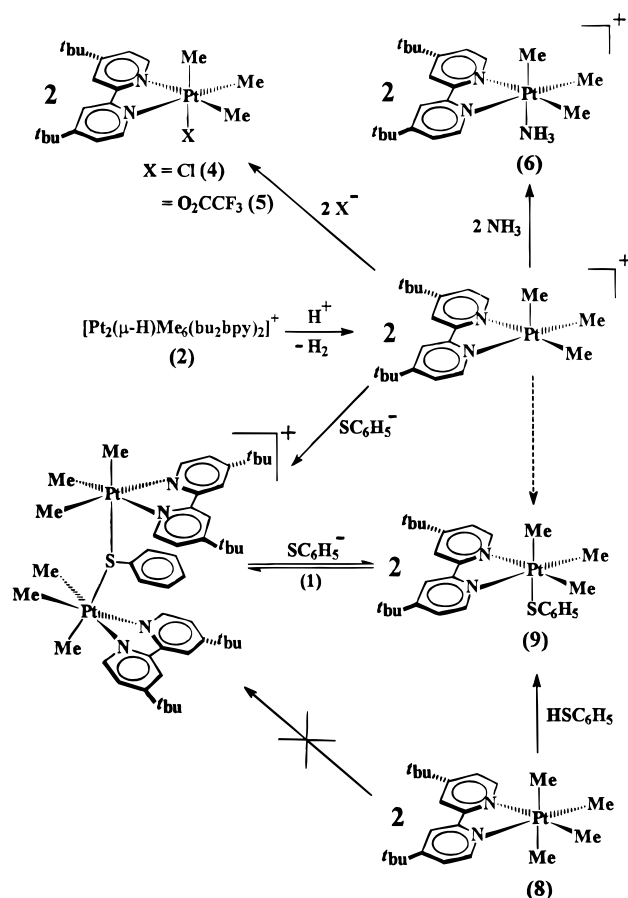
(8) Crabtree, R. H. *The Organometallic Chemistry of the Transition Metals*, 2nd ed.; John Wiley and Sons: New York, 1994.

(9) For example, see: (a) Brown, M. P.; Keith, A. N.; Manojlovic-Muir, L. J.; Muir, K. W.; Puddephatt, R. J.; Seddon, K. R. *Inorg. Chim. Acta* **1979**, 34, L223. (b) Manojlovic-Muir, L. J.; Muir, K. W.; Puddephatt, R. J.; Seddon, K. R. *J. Organomet. Chem.* **1979**, 179, 479. (c) Brown, M. P.; Puddephatt, R. J.; Rashidi, M.; Seddon, K. R. *J. Chem. Soc., Dalton Trans.* **1978**, 1540.

(10) Venanzi, L. M. *Coord. Chem. Rev.* **1982**, 43, 251.

(11) Achar, S.; Scott, J. D.; Vittal, J. J.; Puddephatt, R. J. *Organometallics* **1993**, 12, 4592.

Scheme 3



the detectable platinum(IV) deuteride $[\text{PtD}(\text{Cl})\text{Me}_2(\text{tmeda})]$ and that deuterium incorporation into the methylplatinum groups of $[\text{PtD}(\text{Cl})\text{Me}_2(\text{tmeda})]$ occurs faster than the reductive elimination of methane.^{1a} It was proposed that this occurred by dissociation of the chloride ligand to form a five-coordinate complex as in Scheme 1, followed by easy, reversible formation of a $\text{Pt}(\text{CH}_3\text{D})$ σ -complex. Since neither $\text{fac}[\text{PtDMe}_3(\text{bu}_2\text{bpy})]$ (**3***) nor $[\text{Pt}_2(\mu\text{-D})\text{Me}_6(\text{bu}_2\text{bpy})_2]\text{SO}_3\text{CF}_3$ (**2***) can readily undergo ligand dissociation to form the required five-coordinate intermediate, no isotopic H–D exchange within PtDMe groups would be expected. This prediction was upheld; for example, both the ^1H and $^2\text{H}\{^1\text{H}\}$ NMR spectra of **2*** showed the absence of deuterium incorporation into the MePt groups or of H into the PtD groups, even after several days in solution. This result gives strong support to the theory that these isotopic exchange reactions occur *via* the five-coordinate intermediate $[\text{PtHMe}_2(\text{bu}_2\text{bpy})]^+$.

Reaction of $[\text{Pt}_2(\mu\text{-H})\text{Me}_6(\text{bu}_2\text{bpy})_2]\text{SO}_3\text{CF}_3$ (2**) with Electrophilic Reagents.** The reaction of complex **2** with an excess of HX (HX = HCl, HO_2CCF_3 , NH_4^+ , HSC_6H_5) in acetone- d_6 solution affords either 2 equiv of $\text{fac}[\text{PtClMe}_3(\text{bu}_2\text{bpy})]$ (**4**), $\text{fac}[\text{PtMe}_3(\text{O}_2\text{CCF}_3)(\text{bu}_2\text{bpy})]$ (**5**), and $\text{fac}[\text{Pt}(\text{NH}_3)\text{Me}_3(\text{bu}_2\text{bpy})]\text{SO}_3\text{CF}_3$ (**6**) or 1 equiv of $[\text{Pt}_2\text{Me}_6(\mu\text{-SC}_6\text{H}_5)(\text{bu}_2\text{bpy})_2]\text{SO}_3\text{CF}_3$ (**7**), respectively (Scheme 3). No reaction of HX with the methylplatinum ligands of **2** was observed, and the $\text{fac}[\text{PtMe}_3]$ unit remained intact in all experiments. These reactions proceed very slowly and take several days to reach completion, perhaps due to a combination of the steric protection of the bridging hydride provided by the bu_2bpy ligands and the relatively low hydridic nature of **2** (see earlier). The rates of these reactions are highly

dependent on the acid strength of HX and not the coordinating ability of the conjugate base (X). For example, reactions of **2** with HO_2CCF_3 or HCl are complete within days, whereas a similar reaction with HSC_6H_5 requires several weeks to reach completion, and thiolate is the strongest ligand for platinum. Qualitatively, the rate of these reactions follows the order of the acid strength, i.e. $\text{HCl}, \text{HO}_2\text{CCF}_3 \gg \text{HSC}_6\text{H}_5$, and *not* the order of the ligating ability to platinum of the conjugate base, which would give the sequence $\text{SC}_6\text{H}_5^- > \text{Cl}^- > \text{O}_2\text{CCF}_3^-$. This relationship is consistent with a mechanism that proceeds by slow electrophilic attack of HX or H^+ on **2**, giving H_2 and 2 equiv of $[\text{PtMe}_3(\text{bu}_2\text{bpy})]^+$, followed by a rapid coordination of X^- to give the product (Scheme 3). It has been shown that the electrophilic attack of HX on the tetramethylplatinum(IV) complexes $[\text{PtMe}_4(\text{NN})]$ (NN = 2,2'-bipyridine, 1,10-phenanthroline) to afford CH_4 and $[\text{PtMe}_3\text{X}(\text{NN})]$ proceeds by a similar $[\text{SE}_{2(\text{open})}]$ mechanism.^{2a,12} Note that electrophiles do not attack a methylplatinum group of **2**, again indicating the relatively low *trans*-influence of the bridging hydride ligand. It is possible that electrophiles could attack either the Pt-H group or the MePt group *trans* to H in complex **3**, but since this compound has not been prepared in pure form, no studies have been made.

Complexes **4–7** were characterized by comparing their ^1H NMR spectra to those of authentic samples (see Experimental Section). The ^1H NMR spectra of complexes **4–7** each display the expected three sets of aromatic resonances and one *tert*-butyl resonance due to the two equivalent pyridyl groups of the bu_2bpy ligand. The methylplatinum resonances of complexes **4–7** appear in a 2:1 intensity ratio due to the methylplatinum ligands *trans* to bu_2bpy and *trans* to X, respectively, confirming the presence of the $\text{fac}[\text{PtMe}_3\text{X}(\text{bu}_2\text{bpy})]$ arrangement. These data are summarized in Table 1 and require no further discussion.

The presence of the Pt-NH_3 ligand in complex **6** is supported by a broad resonance in the ^1H NMR spectrum (CD_2Cl_2) at $\delta = 2.30$, which is flanked by quarter-intensity ^{195}Pt satellite signals [$^2J(\text{PtH}) = \text{ca. } 17.5 \text{ Hz}$], due to the NH_3 protons. The ionic nature of **6** is supported by the presence of a singlet at $\delta = -79.0$ in the ^{19}F NMR spectrum (CD_2Cl_2) attributed to the $\text{SO}_3\text{-CF}_3$ anion.

In addition to the expected methylplatinum and *tert*-butyl resonances, the ^1H NMR spectrum (acetone- d_6) of complex **7** displays three sets of resonances at $\delta = 6.55$, 6.11, and 5.43 for the *para*-, *meta*-, and *ortho*-protons of the $\text{Pt-C}_6\text{H}_5$ ligand, respectively. No ^{195}Pt satellite signals were observed. Integration of resonances due to the protons of the SC_6H_5 ligand and the $[\text{PtMe}_3(\text{bu}_2\text{bpy})]$ unit shows that these units are present in a 1:2 ratio, suggesting the presence of a bridging SC_6H_5 ligand (Table 1). The ^{19}F NMR spectrum (acetone- d_6) shows a singlet at -79.0 due to the SO_3CF_3 anion, supporting the ionic nature of **7**. Treatment of **2** with 1 equiv of HSC_6H_5 quantitatively gives complex **7**, strongly supporting the presence of a $(\mu\text{-SC}_6\text{H}_5)$ ligand: a complex with a terminally bound SC_6H_5 ligand would require 2 equiv of HSC_6H_5 to fully react with **2**. The connectivity in **2** has been confirmed by a preliminary X-ray crystal structure determination, but the complex

(12) Kondo, Y.; Ishikawa, M.; Ishihara, K. *Inorg. Chim. Acta* **1996**, *241*, 81.

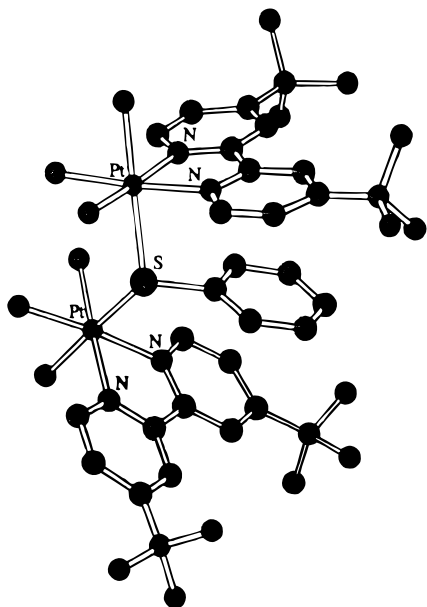


Figure 3. Structure of $[\text{Pt}_2(\mu\text{-SC}_6\text{H}_5)\text{Me}_6(\text{bu}_2\text{bpy})_2]^+$ (**7**) obtained from molecular modeling calculations. The hydrogen atoms have been omitted for clarity.

diffracted weakly and the atoms were not accurately located. A molecular modeling study was performed for the $[\text{Pt}_2(\mu\text{-SC}_6\text{H}_5)\text{Me}_6(\text{bu}_2\text{bpy})_2]^+$ cation, and the predicted structure, shown in Figure 3, is very close to that determined crystallographically. The *syn-syn* arrangement of the $\text{bu}_2\text{bpy-SC}_6\text{H}_5\text{-bu}_2\text{bpy}$ ligands in **7** is similar to that observed for the two bu_2bpy ligands in **2** (Figure 1). By the same argument put forth for **2**, this arrangement in **7** presumably is a result of a π -stacking phenomenon between the aromatic rings of the bu_2bpy and SC_6H_5 ligands.

Interestingly, the tetramethylplatinum(IV) complex $[\text{PtMe}_4(\text{bu}_2\text{bpy})]$ (**8**) reacts with HSC_6H_5 to give *not* complex **7** but *fac*- $[\text{PtMe}_3(\text{SC}_6\text{H}_5)(\text{bu}_2\text{bpy})]$ (**9**) (Scheme 3).¹² No **9** was produced in the reaction of HSC_6H_5 with **2**. The ^1H NMR spectrum (acetone- d_6) of **9** shows three sets of aromatic resonances and one *tert*-butyl resonance due to the bu_2bpy ligand. The methylplatinum resonances appear in the expected 2:1 intensity ratio for the Pt–Me ligands *trans* to bu_2bpy [$\delta = 1.09$, $^2J(\text{PtH}) = 70.6$ Hz] and *trans* to SC_6H_5 [$\delta = 0.15$, $^2J(\text{PtH}) = 63.4$ Hz], respectively. The value of $^2J(\text{PtH})$ for the methylplatinum ligand *trans* to SC_6H_5 in complex **9** (63.4 Hz) is significantly smaller than that in complex **7** (69.3 Hz). Thus the terminal SC_6H_5 ligand in **9** has a larger *trans* influence than the $(\mu\text{-SC}_6\text{H}_5)$ ligand in **7**. This is as expected since the available s-electron density at S must be shared between the two platinum atoms in **7** and only one in **9**. The *para*-, *meta*-, and *ortho*-protons of the Pt– SC_6H_5 ligand resonate at $\delta = 6.56$, 6.35, and 6.32, respectively. Again, no ^{195}Pt satellite signals were observed. Integration of the signals in the ^1H NMR spectrum confirms a terminal SC_6H_5 ligand as the $[\text{PtMe}_3(\text{bu}_2\text{bpy})]$ unit and the SC_6H_5 ligand appear in a 1:1 ratio.

The fact that HSC_6H_5 reacts with **8** to give the terminal SC_6H_5 complex (**9**) but reacts with either **1** or **2** to give the $(\mu\text{-SC}_6\text{H}_5)$ complex (**7**) is fully explained in the mechanism proposed in Scheme 3. For example, if this mechanism is correct, reaction of **2** with 1 equiv of HSC_6H_5 would yield 1 equiv of **9** and 1 equiv of $[\text{PtMe}_3(\text{bu}_2\text{bpy})]^+$. Complex **9** would then rapidly com-

bine with $[\text{PtMe}_3(\text{bu}_2\text{bpy})]^+$ to give **7**. A similar situation most certainly arises when **1** is reacted with HSC_6H_5 to give the stable complex **7** (see Experimental Section). Presumably, **1** initially reacts with HSC_6H_5 to give **9** which then subsequently reacts with additional **1** by displacement of SO_3CF_3 to give **7**. The feasibility of the latter step in this proposed mechanism was confirmed by an independent reaction in which a THF solution of **9** was treated with 1 equiv of complex **1**, immediately producing complex **7** (Scheme 3). Alternatively, the reaction of HSC_6H_5 with $[\text{PtMe}_4(\text{bu}_2\text{bpy})]$ gives **9** and, since there is no readily available source of $[\text{PtMe}_3(\text{bu}_2\text{bpy})]^+$, the reaction proceeds no further.

Complex **2** did not react with other electrophiles such as $[\text{Au}(\text{SO}_3\text{CF}_3)\text{PPh}_3]$ and decomposed to *fac*- $[\text{PtMe}_3(\text{SO}_3\text{CF}_3)(\text{bu}_2\text{bpy})]$ (**1**) upon treatment with $[\text{Hg}(\text{SO}_3\text{CF}_3)_2]$. Unsaturated reagents such as acetylene and dimethyl acetylenedicarboxylate did not react with **2** even after several days in THF solution.

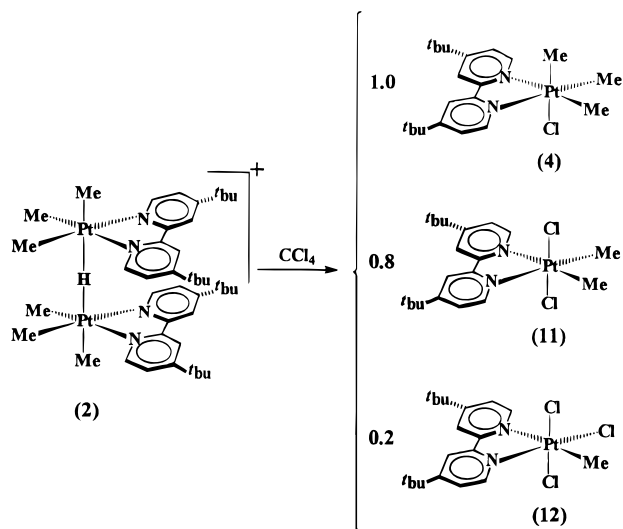
Reaction of $[\text{Pt}_2(\mu\text{-H})\text{Me}_6(\text{bu}_2\text{bpy})_2]\text{SO}_3\text{CF}_3$ (2**) with Nucleophilic Reagents.** Reaction of complex **2** with a large excess of NaBH_4 results in the formation of an equilibrium mixture of **2** and 2 equiv of *fac*- $[\text{PtHMe}_3(\text{bu}_2\text{bpy})]$ (**3**). However, this is not a viable method to synthesize **3** because, under these strongly basic conditions, both complexes slowly decompose with precipitation of metallic platinum. In addition, hydrolytic workup of the reaction mixture leads to decomposition of **3**. Because of this, a detailed investigation of the reaction chemistry of complex **3** has not been possible. Nevertheless, this suggested that the reaction of complex **2** with a more innocent nucleophile (Nu) would yield 1 equiv of **3** and 1 equiv of *fac*- $[\text{PtMe}_3(\text{Nu})(\text{bu}_2\text{bpy})]$. Under these milder conditions, complex **3** should be more stable, potentially allowing a more thorough investigation of **3** to take place.

This prediction was partially upheld; for example the reaction of **2** with excess PPh_3 in refluxing acetone- d_6 solution initially produces 1 equiv of **3** and 1 equiv of *fac*- $[\text{PtMe}_3(\text{PPh}_3)(\text{bu}_2\text{bpy})]\text{SO}_3\text{CF}_3$ (**10**). However, the reaction is exceedingly slow, requiring several weeks to reach completion, and a method to separate complex **3** from **10** and some byproducts formed over the long reaction period has not been found. This experiment clearly indicates that **3** is stable in the absence of electrophiles, and it should be isolable as a pure compound if a better synthetic method can be found.

Complex **10** was characterized by comparing the ^1H NMR spectrum with that of an authentic sample synthesized from *fac*- $[\text{PtMe}_3(\text{SO}_3\text{CF}_3)(\text{bu}_2\text{bpy})]$ and PPh_3 . The ^1H NMR spectrum (acetone- d_6) of **10** shows one *tert*-butyl and three sets of aromatic resonances of the bu_2bpy ligand. The methylplatinum resonances appear in the expected 2:1 intensity ratio for the Pt–Me ligands *trans* to bu_2bpy [$\delta = 1.33$, $^2J(\text{PtH}) = 67.5$ Hz] and *trans* to PPh_3 [$\delta = 0.52$, $^2J(\text{PtH}) = 59.8$ Hz], respectively (Table 1). These values of $^2J(\text{PtH})$ are typical for methylplatinum(IV) ligands *trans* to bu_2bpy and PPh_3 , respectively.⁴ Both methylplatinum signals show coupling to ^{31}P [$^3J(\text{PH}) = \text{ca. } 7.4$ Hz]. The $^{31}\text{P}\{^1\text{H}\}$ NMR spectrum (acetone- d_6) of **10** shows a singlet at $\delta = -2.0$ with quarter-intensity ^{195}Pt satellite signals [$^1J(\text{PtP}) = 994$ Hz].

Other nucleophiles such as halide, hydroxide, $\text{P}(\text{OMe})_3$, and CO were even less reactive than PPh_3 , producing no reaction with **2** even after several weeks in refluxing

Scheme 4



acetone. The stability of complex **2** to nucleophilic attack precludes this methodology as a suitable means of producing **3**.

Reaction of $[\text{Pt}_2(\mu\text{-H})\text{Me}_6(\text{bu}_2\text{bpy})_2]\text{SO}_3\text{CF}_3$ (2**) with CCl_4 .** The reaction of complex **2** with excess CCl_4 gives $\text{fac-}[\text{PtClMe}_3(\text{bu}_2\text{bpy})]$ (**4**), $[\text{PtCl}_2\text{Me}_2(\text{bu}_2\text{bpy})]$ (**11**), and $\text{mer-}[\text{PtCl}_3\text{Me}(\text{bu}_2\text{bpy})]$ (**12**) in a 1.0:0.8:0.2 ratio (Scheme 4), and methane is also formed. This reaction is slow and takes several days to reach completion. Most transition-metal hydrides react with CCl_4 by a free-radical mechanism to give the corresponding metal chloride and CHCl_3 .⁸ The reaction of **2** with CCl_4 does *not* produce CHCl_3 , and a possible explanation for this is presented in the following mechanism. We propose that complex **2** reacts with CCl_4 by an electron-transfer mechanism to give $\text{CCl}_4^{\cdot-}$ and $\mathbf{2}^{+\cdot}$ with further reaction to give CCl_3^{\cdot} , $\text{fac-}[\text{PtClMe}_3(\text{bu}_2\text{bpy})]$ (**4**), and $\text{fac-}[\text{PtHMe}_3(\text{bu}_2\text{bpy})]^+$. This accounts for the 1 equiv of **4** present in the product mixture. The fate of the radical ion $\text{fac-}[\text{PtHMe}_3(\text{bu}_2\text{bpy})]^+$ is uncertain, but presumably it undergoes reductive elimination of methane to give $[\text{PtMe}_2(\text{bu}_2\text{bpy})]^+$ *before* it can further react with CCl_4 . The evolution of CH_3D (with no CH_4) was confirmed by ^1H NMR spectroscopy in a similar reaction using $[\text{Pt}(\mu\text{-D})\text{Me}_6(\text{bu}_2\text{bpy})_2]\text{SO}_3\text{CF}_3$ (**2***). The remaining products, $[\text{PtCl}_2\text{Me}_2(\text{bu}_2\text{bpy})]$ (**11**) and $\text{mer-}[\text{PtCl}_3\text{Me}(\text{bu}_2\text{bpy})]$ (**12**), could then be formed by reaction of $[\text{PtMe}_2(\text{bu}_2\text{bpy})]^+$ with CCl_4 . Only one methylplatinum ligand is present in **12**, and so its formation requires cleavage of a methylplatinum bond at this stage. It is not possible to determine how this happens, but the use of CCl_4 as a source of chlorine in oxidative addition is not unexpected.

Complexes **11** and **12** were characterized by comparing the ^1H NMR spectra to those of the authentic samples prepared by the *trans* oxidative addition of Cl_2 to $[\text{PtMe}_2(\text{bu}_2\text{bpy})]$ and $[\text{PtClMe}(\text{bu}_2\text{bpy})]$, respectively (see Experimental Section).

The ^1H NMR spectrum (acetone- d_6) of complex **11** displays one methylplatinum resonance [$\delta = 1.85$, $^2J(\text{PtH}) = 69.5$] and three sets of bu_2bpy aromatic resonances (Table 1). This value of $^2J(\text{PtH})$ is consistent with a methylplatinum(IV) ligand *trans* to bu_2bpy . These data support the proposed stereochemistry for **11** in which the chloride ligands are mutually *trans* and rules out all alternative isomers. The ^1H NMR spec-

trum (acetone- d_6) of complex **12** displays six sets of aromatic resonances and one *tert*-butyl resonance suggesting inequivalent pyridyl groups of the bu_2bpy ligand. This supports the *mer*-arrangement of the three chloride ligands of complex **12** and rules out the alternative isomer $\{\text{fac-}[\text{PtCl}_3\text{Me}(\text{bu}_2\text{bpy})]\}$ in which the pyridyl groups would be equivalent. The methylplatinum ligands of complexes **11** and **12** resonate at uncharacteristically high frequencies ($\delta = 1.85$ and 2.69 , respectively), and this is caused by a deshielding effect of the neighboring electronegative Cl atoms.

Conclusions

The new methyl(hydrido)platinum(IV) complexes $[\text{Pt}_2(\mu\text{-H})\text{Me}_6(\text{bu}_2\text{bpy})_2]\text{SO}_3\text{CF}_3$ (**2**) and $\text{fac-}[\text{PtHMe}_3(\text{bu}_2\text{bpy})]$ (**3**) are thermally stable to reductive elimination of CH_4 and to isotopic exchange within $\text{Pt}(\text{D})\text{CH}_3$ groups. This gives strong support to the theory that both reactions proceed through a common, five-coordinate intermediate $[\text{PtHMe}_2(\text{bu}_2\text{bpy})]^+$. Complex **2** exhibits only moderate reactivity to a variety of reagents with all reactions occurring at the μ -hydrido ligand. This behavior of **2** is due to a combination of the steric protection of the hydrido ligand by bu_2bpy and the reduced hydridic nature of **2**.

Experimental Section

General Procedures. All reactions were performed under a N_2 atmosphere using standard Schlenk techniques, unless otherwise stated. All solvents were freshly distilled, dried, and degassed prior to use. CCl_4 was refluxed over P_4O_{10} and distilled prior to use. NMR spectra were recorded using a Varian Gemini spectrometer (^1H at 300.10 MHz, ^{19}F at 282.32 MHz, ^{31}P at 121.44 MHz, ^{195}Pt at 42.99 MHz, and ^2H at 30.70 MHz). Chemical shifts are reported in ppm with respect to TMS (^1H and ^2H), CFCl_3 (^{19}F), $\text{H}_3\text{PO}_4/\text{D}_2\text{O}$ (^{31}P), or $\text{K}_2[\text{PtCl}_4]/\text{D}_2\text{O}$ (^{195}Pt). The ^1H , ^2H , ^{19}F , ^{31}P , and ^{195}Pt NMR spectra are referenced to the residual protons of the deuterated solvents or to deuterated solvents, CFCl_3 , $\text{H}_3\text{PO}_4/\text{D}_2\text{O}$, or $\text{K}_2[\text{PtCl}_4]/\text{D}_2\text{O}$ contained in a coaxial insert, respectively. IR spectra (Nujol mull) were recorded in the range 4000–400 cm^{-1} using a Perkin-Elmer 2000 FT-IR instrument. Elemental analyses were determined by Guelph Chemical Laboratories, Guelph, Canada. Thermogravimetric (TGA) studies were performed using a Perkin-Elmer TGA 7 thermogravimetric analyzer equipped with a Perkin-Elmer TAC 7/DX thermal analysis controller. Samples for TGA analysis were heated in platinum pans under a N_2 atmosphere in the range 20–1000 $^\circ\text{C}$ at a rate of 20 $^\circ\text{C}/\text{min}$. Molecular mechanics calculations were performed using the CAChe version 3.8 software package employing MM2 force-field parameters and a conjugate gradient optimization method.

The complexes $[\text{PtMe}_2(\text{bu}_2\text{bpy})]$,¹¹ $[\text{PtMeCl}(\text{bu}_2\text{bpy})]$,¹⁴ and $[\text{Pt}_2\text{Me}_8(\mu\text{-SMe}_2)_2]$ ¹⁵ were synthesized according to literature procedures. The syntheses for complexes $\text{fac-}[\text{PtClMe}_3(\text{bu}_2\text{bpy})]$ (**4**), $\text{fac-}[\text{PtIME}_3(\text{bu}_2\text{bpy})]$, $\text{fac-}[\text{PtMe}_3(\text{O}_2\text{CCF}_3)(\text{bu}_2\text{bpy})]$ (**5**), $[\text{PtMe}_4(\text{bu}_2\text{bpy})]$ (**8**), and $\text{fac-}[\text{PtMe}_3(\text{SC}_6\text{H}_5)(\text{bu}_2\text{bpy})]$ (**9**) are modified versions of those published for the bpy (bpy = 2,2'-bipyridine) analogues.^{2a,16}

Preparation of Complexes. $\text{fac-}[\text{PtMe}_3(\text{SO}_3\text{CF}_3)(\text{bu}_2\text{bpy})]$ (**1**). To a suspension of $[\text{PtMe}_2(\text{bu}_2\text{bpy})]$ (1.73 g, 3.51 mmol) in diethyl ether (40.0 mL) was added $\text{MeOSO}_2\text{CF}_3$

(13) For the analogous reaction with $[\text{PtMe}_4(\text{bpy})]$ see ref 2a.

(14) Rendina, L. M.; Vittal, J. J.; Puddephatt, R. J. *Organometallics* **1995**, *14*, 1030.

(15) Lashanizadehgan, M.; Rashidi, R.; Hux, J. E.; Puddephatt, R. J.; Ling, S. S. M. *J. Organomet. Chem.* **1984**, *269*, 317.

(16) Clegg, D. E.; Hall, J. R.; Swile, G. A. *J. Organomet. Chem.* **1972**, *38*, 1532.

(0.400 mL, 3.53 mmol) producing an immediate bright orange to pale yellow color change. After the solution was stirred under a N₂ atmosphere for 18 h, the solvent was removed *in vacuo* to give an off-white powder. Yield: 2.30 g (99%). Anal. Calcd for C₂₂H₃₃F₃N₂O₃PtS: C, 40.2; H, 5.0; N, 4.2. Found: C, 40.2; H, 4.8; N, 3.9. ¹H NMR in acetone-*d*₆: δ = 8.90 [d, 2H, ³J(H⁶H⁵) = 5.7 Hz, ³J(PtH) = *ca.* 14.0 Hz, H⁶], 8.80 [d, 2H, ⁴J(H³H⁵) = 2.0 Hz, H³], 7.97 [dd, 2H, ⁴J(H⁵H³) = 2.0 Hz, ³J(H⁵H⁶) = 5.7 Hz, H⁵], 1.49 [s, 18H, ⁴bu], 1.21 [s, 6H, ²J(PtH) = 66.5 Hz, Pt–Me (*trans* to bu₂bpy)], 0.64 [s, 3H, ²J(PtH) = 87.0 Hz, Pt–Me (*trans* to SO₃CF₃)]. ¹⁹F NMR in acetone-*d*₆: δ = –79 [s].

[Pt₂(μ-H)Me₆(bu₂bpy)₂](SO₃CF₃) (2). To a solution of *fac*-[PtMe₃(SO₃CF₃)(bu₂bpy)] (300 mg, 0.456 mmol) in THF (200 mL) was slowly added a solution of NaBH₄ (17.3 mg, 0.456 mmol) in THF (100 mL). The resulting amber solution was stirred under a N₂ atmosphere for 18 h. Removal of the solvent *in vacuo* gave a dark brown solid. This solid was then triturated with *n*-pentane (3 × 50 mL) to give a pale brown powder from which the product was extracted with CH₂Cl₂ (60 mL). The CH₂Cl₂ extract was then filtered through Celite filter-aid giving a bright-yellow solution. The solvent was removed *in vacuo* to afford a yellow powder. Yield: 220 mg (83%). Anal. Calcd for C₄₃H₆₇F₃N₄O₃Pt₂S₂: C, 44.3; H, 5.8; N, 4.8. Found: C, 44.4; H, 5.7; N, 4.8. ¹H NMR in CD₂Cl₂: δ = 8.21 [d, 4H, ³J(H⁶H⁵) = 6.3 Hz, ³J(PtH) = 14.0 Hz, H⁶], 8.09 [d, 4H, ⁴J(H³H⁵) = 2.0 Hz, H³], 7.51 [dd, 4H, ⁴J(H⁵H³) = 1.9 Hz, ³J(H⁵H⁶) = 6.2 Hz, H⁵], 1.49 [s, 36H, ⁴bu], 0.47 [s, 12H, ²J(PtH) = 69.6 Hz, ³J(HH) = *ca.* 1.0 Hz, Pt–Me (*trans* to bu₂bpy)], 0.13 [s, 6H, ²J(PtH) = 65.9 Hz, ³J(HH) = *ca.* 1.0 Hz, Pt–Me (*trans* to H)], –11.7 [s, 1H, ¹J(PtH) = 442 Hz, Pt–H]; ¹⁹⁵Pt NMR in THF-*d*₈: δ = –1238 [d, ¹J(PtH) = 440 Hz]. ¹⁹F NMR CD₂Cl₂: δ = –79 [s].

When a similar reaction of *fac*-[PtMe₃(SO₃CF₃)(bu₂bpy)] with NaBH₄ was carried out in THF-*d*₈, monitoring by NMR showed the presence of both **2** and **3** in solution, the relative concentration of **3** increasing with the amount of NaBH₄ added. ¹H NMR in THF-*d*₈: δ = 8.44 [d, 2H, ⁴J(H³H⁵) = 2.0 Hz, H³], 8.24 [d, 2H, ³J(H⁶H⁵) = 6.0 Hz, H⁶], 7.64 [dd, 2H, ⁴J(H⁵H³) = 2.0 Hz, ³J(H⁵H⁶) = 6.0 Hz, H⁵], 1.52 [s, 18H, ⁴bu], 0.01 [s, 6H, ²J(PtH) = 65.7 Hz, Pt–Me (*trans* to bu₂bpy)], –0.74 [s, 3H, ²J(PtH) = 44.0 Hz, Pt–Me (*trans* to H)], –7.0 [s, 1H, ¹J(PtH) = 805 Hz, Pt–H].

***fac*-[PtClMe₃(bu₂bpy)] (4).** A solution of *fac*-[PtMe₃(SO₃CF₃)(bu₂bpy)] (100 mg, 0.152 mmol) and LiCl (7.5 mg, 0.177 mmol) in THF (10.0 mL) was stirred under a N₂ atmosphere for 24 h. Removal of the solvent *in vacuo* gave a pale-yellow residue from which the product was extracted with CH₂Cl₂ (2 × 5 mL). The CH₂Cl₂ extracts were combined and filtered through Celite filter-aid to afford a pale-yellow filtrate. Removal of the solvent *in vacuo* gave a yellow powder. Yield: 81 mg (98%). Anal. Calcd for C₂₁H₃₃ClN₂Pt: C, 46.4; H, 6.1; N, 5.2. Found: C, 46.7; H, 5.9; N, 5.1. ¹H NMR in acetone-*d*₆: δ = 8.79 [d, 2H, ³J(H⁶H⁵) = 5.9 Hz, ³J(PtH) = *ca.* 14.0 Hz, H⁶], 8.69 [d, 2H, ⁴J(H³H⁵) = 2.0 Hz, H³], 7.84 [dd, 2H, ⁴J(H⁵H³) = 2.0 Hz, ³J(H⁵H⁶) = 5.9 Hz, H⁵], 1.46 [s, 18H, ⁴bu], 1.99 [s, 6H, ²J(PtH) = 69.7 Hz, Pt–Me (*trans* to bu₂bpy)], 0.36 [s, 3H, ²J(PtH) = 74.5 Hz, Pt–Me (*trans* to Cl)].

***fac*-[PtIme₃(bu₂bpy)] (5).** To a solution of [PtMe₂(bu₂bpy)] (400 mg, 0.810 mmol) in acetone (20.0 mL) was added an excess of MeI (*ca.* 0.25 mL) producing an immediate bright-orange to pale-yellow color change. The solvent was removed *in vacuo* giving a yellow solid. Yield: 514 mg (99%). Anal. Calcd for C₂₁H₃₃IN₂Pt: C, 39.7; H, 5.2; N, 4.4. Found: C, 40.1; H, 5.4; N, 4.5. ¹H NMR in acetone-*d*₆: δ = 8.87 [d, 2H, ³J(H⁶H⁵) = 5.7 Hz, ³J(PtH) = *ca.* 14.5 Hz, H⁶], 8.70 [d, 2H, ⁴J(H³H⁵) = 1.8 Hz, H³], 7.82 [dd, 2H, ⁴J(H⁵H³) = 1.8 Hz, ³J(H⁵H⁶) = 5.7 Hz, H⁵], 1.47 [s, 18H, ⁴bu], 1.42 [s, 6H, ²J(PtH) = 70.6 Hz, Pt–Me (*trans* to bu₂bpy)], 0.54 [s, 3H, ²J(PtH) = 73.5 Hz, Pt–Me (*trans* to I)].

***fac*-[PtMe₃(O₂CCF₃)(bu₂bpy)] (5).** A solution of *fac*-[PtIme₃(bu₂bpy)] (103 mg, 0.162 mmol) and AgO₂CCF₃ (35.8 mg, 0.162 mmol) in CH₂Cl₂ (10.0 mL) was stirred under a N₂

atmosphere in the absence of light for 2 h. After filtration of the mixture through Celite filter-aid, the solvent of the pale-yellow filtrate was removed to give a yellow powder. Yield: 100 mg (99%). Anal. Calcd for C₂₃H₃₃F₃N₂O₂Pt: C, 44.7; H, 5.0; N, 4.9. Found: C, 44.8; H, 5.3; N, 4.5. ¹H NMR in acetone-*d*₆: δ = 8.88 [d, 2H, ³J(H⁶H⁵) = 6.0 Hz, ³J(PtH) = *ca.* 13.5 Hz, H⁶], 8.69 [d, 2H, ⁴J(H³H⁵) = 2.0 Hz, H³], 7.84 [dd, 2H, ⁴J(H⁵H³) = 2.0 Hz, ³J(H⁵H⁶) = 6.0 Hz, H⁵], 1.46 [s, 18H, ⁴bu], 1.98 [s, 6H, ²J(PtH) = 67.4 Hz, Pt–Me (*trans* to bu₂bpy)], 0.34 [s, 3H, ²J(PtH) = 76.4 Hz, Pt–Me (*trans* to O₂CCF₃)]. ¹⁹F NMR in acetone-*d*₆: δ = –74 [s].

***fac*-[Pt(NH₃)Me₃(bu₂bpy)]SO₃CF₃ (6).** An NH₃-saturated solution (1 atm) of *fac*-[PtMe₃(SO₃CF₃)(bu₂bpy)] (100 mg, 0.152 mmol) in CH₂Cl₂ (10.0 mL) was stirred for 30 min producing a pale-yellow to colorless color change. The solvent was removed *in vacuo* to give a white powder. The product can be recrystallized from CH₂Cl₂/*n*-pentane to give a white microcrystalline solid. Yield: 100 mg (97%). Anal. Calcd for C₂₂H₃₇F₃N₃O₃PtS: C, 39.2; H, 5.4; N, 6.2. Found: C, 39.1; H, 5.4; N, 6.5. ¹H NMR in CD₂Cl₂: δ = 8.70 [d, 2H, ³J(H⁶H⁵) = 6.0 Hz, ³J(PtH) = *ca.* 14.0 Hz, H⁶], 8.25 [d, 2H, ⁴J(H³H⁵) = 2.1 Hz, H³], 7.70 [dd, 2H, ⁴J(H⁵H³) = 2.1 Hz, ³J(H⁵H⁶) = 6.0 Hz, H⁵], 2.30 [br s, 3H, ²J(PtH) = *ca.* 17.5 Hz, Pt–NH₃], 1.47 [s, 18H, ⁴bu], 1.04 [s, 6H, ²J(PtH) = 67.8 Hz, Pt–Me (*trans* to bu₂bpy)], 0.31 [s, 3H, ²J(PtH) = 71.5 Hz, Pt–Me (*trans* to NH₃)]. ¹⁹F NMR in CD₂Cl₂: δ = –79.0 [s].

[Pt₂Me₆(μ-SC₆H₅)(bu₂bpy)₂](SO₃CF₃) (7). A solution of *fac*-[PtMe₃(SO₃CF₃)(bu₂bpy)] (200 mg, 0.304 mmol) and C₆H₅SH (32 mL, 0.312 mmol) in CH₂Cl₂ (6.0 mL) was stirred over anhydrous K₂CO₃ for 18 h. This bright-yellow solution was then filtered through Celite filter-aid. The solvent of the filtrate was then removed *in vacuo* yielding a yellow oil which, after trituration with *n*-pentane (20.0 mL), gave a bright yellow powder. Yield: 150 mg (78%). Anal. Calcd for C₄₉H₇₁F₃N₄O₃Pt₂S₂: C, 46.1; H, 5.6; N, 4.4. Found: C, 46.1; H, 5.6; B, 4.3. ¹H NMR in acetone-*d*₆: δ = 8.56 [d, 4H, ³J(H⁶H⁵) = 6.0 Hz, ³J(PtH) = 13.7 Hz, H⁶], 8.27 [d, 4H, ⁴J(H³H⁵) = 1.9 Hz, H³], 7.70 [dd, 4H, ⁴J(H⁵H³) = 1.9 Hz, ³J(H⁵H⁶) = 5.9 Hz, H⁵], 6.55 [t, 1H, ³J(H²H³) = 7.6 Hz, *p*-SC₆H₅], 6.11 [dd, 2H, ³J(H²H³) = 7.6 Hz, ³J(H²H⁴) = 7.6 Hz, *m*-SC₆H₅], 5.43 [d, 2H, ³J(H²H³) = 7.6 Hz, *o*-SC₆H₅], 1.37 [s, 36H, ⁴bu], 1.15 [s, 12H, ²J(PtH) = 69.3 Hz, Pt–Me (*trans* to bu₂bpy)], 0.36 [s, 6H, ²J(PtH) = 69.8 Hz, Pt–Me (*trans* to SC₆H₅)]. ¹⁹F NMR in acetone-*d*₆: δ = –79 [s].

[PtMe₄(bu₂bpy)] (8). A solution of [Pt₂Me₆(μ-SMe₂)₂] (0.78 g, 1.23 mmol) and bu₂bpy (0.66 g, 2.45 mmol) in diethyl ether (40.0 mL) was stirred for 15 min under a N₂ atmosphere. The solvent was removed from the solution *in vacuo* to give a bright-orange powder. Yield: 1.28 g (99%). Anal. Calcd for C₂₂H₃₆N₂Pt: C, 50.5; H, 6.9; N, 5.4. Found: C, 50.6; H, 7.0; N, 5.3. ¹H NMR in acetone-*d*₆: δ = 8.77 [d, 2H, ³J(H⁶H⁵) = 6.0 Hz, ³J(PtH) = *ca.* 14.0 Hz, H⁶], 8.64 [d, 2H, ⁴J(H³H⁵) = 1.7 Hz, H³], 7.72 [dd, 2H, ⁴J(H⁵H³) = 1.9 Hz, ³J(H⁵H⁶) = 5.9 Hz, H⁵], 1.49 [s, 18H, ⁴bu], 0.84 [s, 6H, ²J(PtH) = 72.0 Hz, Pt–Me (*trans* to bu₂bpy)], 0.65 [s, 3H, ²J(PtH) = 44.0 Hz, Pt–Me (*trans* to Me)].

***fac*-[PtMe₃(SC₆H₅)(bu₂bpy)] (9).** A solution of [PtMe₄(bu₂bpy)] (70 mg, 0.134 mmol) and C₆H₅SH (14 mL, 0.14 mmol) in acetone (5.0 mL) was stirred under a N₂ atmosphere for 24 h producing a yellow solution. Evaporation of the solvent *in vacuo* gave a bright-yellow powder. Yield: 82.7 mg (99%). Anal. Calcd for C₂₇H₃₈N₂PtS: C, 52.5; H, 6.2; N, 4.5. Found: C, 52.6; H, 6.1; N, 4.4. ¹H NMR in acetone-*d*₆: δ = 8.65 [d, 2H, ³J(H⁶H⁵) = 5.9 Hz, ³J(PtH) = *ca.* 13 Hz, H⁶], 8.26 [d, 2H, ⁴J(H³H⁵) = 2.0 Hz, H³], 7.70 [dd, 2H, ⁴J(H⁵H³) = 2.0 Hz, ³J(H⁵H⁶) = 5.9 Hz, H⁵], 6.56 [m, 1H, *p*-SC₆H₅], 6.35 [m, 2H, *m*-SC₆H₅], 6.32 [m, 2H, *o*-SC₆H₅], 1.43 [s, 18H, ⁴bu], 1.09 [s, 6H, ²J(PtH) = 70.6 Hz, Pt–Me (*trans* to bu₂bpy)], 0.15 [s, 3H, ²J(PtH) = 63.4 Hz, Pt–Me (*trans* to SC₆H₅)].

***fac*-[PtMe₃(PPh₃)(bu₂bpy)]SO₃CF₃ (10).** A solution of *fac*-[PtMe₃(SO₃CF₃)(bu₂bpy)] (100 mg, 0.152 mmol) and PPh₃

Table 3. Crystallographic Details for 2·THF

empirical formula	C ₄₇ H ₇₅ F ₃ N ₄ O ₄ Pt ₂ S
fw	1239.35
temp	24 °C
wavelength	0.71073 Å
cryst system	monoclinic
space group	C2/c
unit cell dimens	<i>a</i> = 47.307(7) Å, <i>b</i> = 12.758(1) Å, <i>c</i> = 18.186(3) Å, β = 105.0(1)°
<i>V</i>	10602(3) Å ³
<i>Z</i>	8
<i>D</i> _{calcd}	1.553 g·cm ⁻³
abs coeff	5.364 mm ⁻¹
indepdt reflns	7257 (<i>R</i> (int) = 0.0400)
refinement method	full-matrix least-squares on <i>F</i> ²
data/restraints/params	4343/342/429
goodness-of-fit (<i>GooF</i>) ^a on <i>F</i> ²	1.007
final <i>R</i> indices [<i>I</i> > 2 σ (<i>I</i>)]	<i>R</i> 1 = 0.0602, <i>wR</i> 2 = 0.1312
<i>R</i> indices (all data) ^a	<i>R</i> 1 = 0.1195, <i>wR</i> 2 = 0.1643

^a *R*1 = $\Sigma(|F_o| - |F_c|)/\Sigma|F_o|$. *wR*2 = $[\Sigma w(F_o^2 - F_c^2)^2/\Sigma wF_o^4]^{1/2}$. *GooF* = $[\Sigma w(F_o^2 - F_c^2)^2/(n - p)]^{1/2}$, where *n* is the number of reflections and *p* is the number of parameters refined.

(40 mg, 0.152 mmol) in CH₂Cl₂ (10.0 mL) was stirred under a N₂ atmosphere for 3 h. The solvent was removed *in vacuo* giving a white powder. Yield: 139 mg (99%). Anal. Calcd for C₄₀H₄₈F₃N₂O₃PtS: C, 52.2; H, 5.3; N, 3.0. Found: C, 52.0; H, 5.0; N, 2.6. ¹H NMR in acetone-*d*₆: δ = 8.65 [d, 2H, ³*J*(H³H⁵) = 2.0 Hz, H³], 8.42 [d, 2H, ³*J*(H⁶H⁵) = 6.3 Hz, ³*J*(PtH) = *ca.* 13.5 Hz, H⁶], 7.75 [dd, 2H, ⁴*J*(H⁵H³) = 2.0 Hz, ³*J*(H⁵H⁶) = 6.2 Hz, H⁵], 7.44 [m, 3H, Pt–PPh₃], 7.31 [m, 6H, Pt–PPh₃], 7.09 [m, 6H, Pt–PPh₃], 1.44 [s, 18H, ⁴bu], 1.33 [s, 6H, ²*J*(PtH) = 67.5 Hz, ³*J*(PH) = 7.4 Hz, Pt–Me (*trans* to bu₂bpy)], 0.52 [s, 3H, ²*J*(PtH) = 59.8 Hz, ³*J*(PH) = 7.3 Hz, Pt–Me (*trans* to PPh₃)]. ³¹P{¹H} NMR in acetone-*d*₆: δ = –2.0 [s, ¹*J*(PtP) = 99.4 Hz]. ¹⁹F NMR in acetone-*d*₆: δ = –79.0 [s].

[PtCl₂Me₂(bu₂bpy)] (11). A Cl₂-saturated solution (1 atm) of [PtMe₂(bu₂bpy)] (100 mg, 0.203 mmol) in CH₂Cl₂ (5.0 mL) was stirred for 5 min producing an immediate bright-orange to yellow color change. The solvent was removed *in vacuo* giving a pale yellow powder. Yield: 114 mg (99%). Anal. Calcd for C₂₀H₃₀Cl₂N₂Pt: C, 42.6; H, 5.4; N, 5.0. Found: C, 42.4; H, 5.3; N, 4.8. ¹H NMR in acetone-*d*₆: δ 8.84 [d, 2H, ³*J*(H⁶H⁵) = 5.9 Hz, ³*J*(PtH) = *ca.* 13 Hz, H⁶], 8.74 [d, 2H, ⁴*J*(H³H⁵) = 1.9 Hz, H³], 7.90 [dd, 2H, ⁴*J*(H⁵H³) = 1.9 Hz, ³*J*(H⁵H⁶) = 5.9 Hz, H⁵], 1.85 [s, 6H, ²*J*(PtH) = 69.5 Hz, Pt–Me], 1.46 [s, 18H, ⁴bu].

mer-[PtCl₃Me(bu₂bpy)] (12). A Cl₂-saturated solution (1 atm) of [PtClMe(bu₂bpy)] (100 mg, 0.194 mmol) in CH₂Cl₂ (5.0 mL) was stirred for 20 min. The solvent was removed *in vacuo* giving a bright-yellow powder. Yield: 113 mg (99%). Anal. Calcd for C₁₉H₂₇Cl₃N₂Pt: C, 39.0; H, 4.6; N, 4.8. Found: C, 39.3; H, 4.7; N, 4.6. ¹H NMR in acetone-*d*₆: δ 9.34 [d, 1H, ³*J*(H⁶H⁵) = 6.0 Hz, ³*J*(PtH) = 12.0 Hz, H⁶], 8.84 [d, 1H, ⁴*J*(H³H⁵) = 2.0 Hz, H³], 8.82 [d, 1H, ³*J*(H⁶H⁵) = 6.0 Hz, H⁶], 8.81 [d, 1H, ⁴*J*(H³H⁵) = 2.0 Hz, H³], 8.08 [dd, 1H, ⁴*J*(H⁵H³) = 2.0 Hz, ³*J*(H⁵H⁶) = 6.0 Hz, H⁵], 7.98 [dd, 1H, ⁴*J*(H⁵H³) = 2.0 Hz, ³*J*(H⁵H⁶) = 6.0 Hz, H⁵], 2.69 [s, 3H, ²*J*(PtH) = 68.0 Hz, Pt–Me], 1.50 [s, 9H, ⁴bu], 1.49 [s, 9H, ⁴bu].

Reactions of 2 with Acids. NMR solutions (acetone-*d*₆) of **2** and 2 equiv of either HCl (obtained from Me₃SiCl and H₂O), HO₂CCF₃, or HSC₆H₅ were monitored by ¹H NMR spectroscopy over the period of several days. The extent of reaction was measured by integrating the methylplatinum resonances of **2** relative to those of **4**, **5**, or **7**, respectively. The qualitative rate follows the order of HCl \approx HO₂CCF₃ \gg HSC₆H₅.

Reaction of 2 with CCl₄. An NMR solution (acetone-*d*₆) of **2** and a 4-fold excess of CCl₄ was monitored by ¹H NMR spectroscopy. The reaction was complete after *ca.* 4 days giving **4**, **11**, and **12** in a 1.0:0.8:0.2 product ratio. Chloroform was not detected by ¹H NMR spectroscopy.

Crystal Structure Analysis of [Pt₂(μ -H)Me₆(bu₂bpy)₂]-SO₃CF₃·1.0THF. Large yellow platelike crystals were obtained from a mixture of THF and *n*-pentane by slow diffusion method. A large plate was cut to the size 0.33 \times 0.27 \times 0.23 mm, mounted inside a Lindemann capillary tube, flame sealed, and used for the diffraction experiments. The diffraction experiments were carried out using a Siemens P4 diffractometer with XSCANS software package using graphite-monochromated Mo K α radiation at 24 °C.¹⁷ The cell constants were obtained by centering 25 high-angle reflections ($11.2 \leq 2\theta \leq 25.0^\circ$). A total of 8085 reflections were collected in the θ range 1.66–23.03° ($-1 \leq h \leq 51$, $-1 \leq k \leq 14$, $-19 \leq l \leq 19$) in ω -scan mode at variable scan speeds (2–30 deg/min). Background measurements were made at the ends of the scan range. Four standard reflections were monitored at the end of every 296 reflections. An empirical absorption was applied to the data on the basis of ψ -scan techniques. The minimum and maximum transmission factors are 0.258 and 0.406. The systematic absences indicated that the space group could be either *Cc* or *C2/c*. For *Z* = 8, in the monoclinic system, the space group *C2/c* was chosen. The correctness of the choice of the space group was confirmed by successful solution and refinement of the structure. SHELXTL programs were used for data processing and the least-squares refinements on *F*².¹⁸ All the Pt and the carbon atoms of the methyl and *tert*-butyl atoms were refined anisotropically. Isotropic thermal parameters were refined for the atoms in the bipyridyl rings. The methyl atoms of the *tert*-butyl carbon C(6c) were found to be disordered. Two orientations were resolved (0.6/0.4). Common isotropic thermal parameters were refined for each of these models. Soft constraints were applied for all the *tert*-butyl groups using the option SADI. The SO₃CF₃[–] anion was disordered. Two disorder models (occupancy 0.6/0.4) were included in the least-squares refinements. The geometry of the two models was idealized using the option DFIX. Common isotropic thermal parameters were refined for each model. A region of electron density was found in the difference Fourier, and this was recognized to be tetrahydrofuran (THF) having three different orientations in the crystal lattice. Again, each model was idealized and included in the least-squares refinements. Common isotropic thermal parameters were refined for each model. No attempt was made to locate all the hydrogen atoms. However, the hydrogen atom near the Pt atoms was located successfully in the difference Fourier. Only the positional parameter was refined with a soft constraint imposed that the Pt–H be equal using SADI, and temperature factor was fixed at *U* = 0.05 Å². All the hydrogen atoms were placed in calculated ideal positions for the purpose of structure factor calculations only. In the final least-squares refinement cycles on *F*², the model converged at *R*1 = 0.0602, *wR*2 = 0.1312, and *GooF* = 1.007, for 4343 observations with *F*_o \geq 4 σ (*F*_o) and 429 parameters, and *R*1 = 0.1195 and *wR*2 = 0.1643, for all 7257 data. In the final difference Fourier synthesis, the electron density fluctuates in the range 1.094 to –0.882 e Å^{–3}. The mean shift/esd and the maximum shift in the final cycles are 0.005 and –0.090, respectively. A secondary extinction correction was refined to be 0.000 076(13).

Supporting Information Available: Tables of crystal data, complete positional and thermal parameters of the non-hydrogen atoms, bond distances and angles, hydrogen atom coordinates, selected weighted least-squares planes, and selected dihedral angles for **2**·THF (14 pages). Ordering information is given on any current masthead page.

OM960975L

(17) XSCANS version 2.1; Siemens Analytical X-Ray Instruments Inc.: Madison, WI, 1994.

(18) SHELXTL Software version 5.0; Siemens Analytical X-Ray Instruments Inc.: Madison, WI, 1994.